Retinal Nerve Fiber Layer Split Bundles Are True Anatomic Variants

Ehud Kaliner, MD, Matan J. Cohen, MD, MPH, Hagai Miron, DMD, Michael Kogan, PhD, Eytan Z. Blumenthal, MD

Purpose: The presence of retinal nerve fiber layer (RNFL) split bundles recently was described in normal eyes scanned using scanning laser polarimetry. In this study, the authors set out to ascertain whether RNFL split bundles can be found in histologic sections of normal human eyes.

Design: Histologic study of postmortem human eyes.

Participants: Fourteen normal postmortem eyes obtained from 13 individuals.

Methods: Peripapillary RNFL thickness measurements were plotted, for each eye, from ring sections of 3.0, 3.5, 4.0, and 4.5 mm in diameter. The presence of superior or inferior split RNFL patterns, or both, was sought.

Main Outcome Measures: The presence of superior or inferior split bundles or both in the histologic data.

Results: Five of 14 eyes demonstrated a distinct histologic pattern of RNFL split bundles, of which 3 were found superiorly and 2 inferiorly. None of these 14 eyes demonstrated both a definite superior and a definite inferior split.

Conclusions: This study provides histologic evidence demonstrating that RNFL split bundles are likely a true anatomic finding, rather than an imaging artifact, and that their presence seems to be relatively common in normal eyes. The presence of a split bundle, being a normal variant, should be distinguished from RNFL loss.
Ophthalmology 2007;114:2259–2264 © 2007 by the American Academy of Ophthalmology.

In healthy eyes, the peripapillary retinal nerve fiber layer (RNFL) thickness modulation pattern around the optic disc, also referred to as a temporal-superior-nasal-inferior-temporal graph was shown on imaging to follow a double-hump pattern, with thicker RNFL superiorly and inferiorly and thinner RNFL temporally and nasally.[1,2] Colen and Lemij[3] presented GDx fixed corneal compensation data demonstrating that in a significant proportion of normal eyes examined using scanning laser polarimetry (Carl Zeiss Meditec, Dublin, CA; formerly Laser Diagnostic Technologies, San Diego, CA) showed the presence of split superior and inferior bundles, thus transforming the peripapillary RNFL thickness modulation in some eyes into a triple (or even a quadruple) hump pattern. From 454 normal eyes of 254 healthy white persons examined in that study, 6.4% of the eyes demonstrated a clear split superior bundle pattern, 1.1% demonstrated a clear split inferior bundle pattern, and 0.2% (1 eye) demonstrated with both superior and inferior split bundles. In total, they conclude that 12% of 254 healthy subjects were found to have a superior split bundle in one, or both, of their eyes. An earlier publication by Pieroth et al[4] also described a split bundle pattern in a single healthy eye imaged using optical coherence tomography.

Strengthening the observation of Colen and Lemij,[3] the normative database-derived values of the normal RNFL thickness range for both the GDx variable corneal compensation as well as the StratusOCT (Carl Zeiss Meditec), as seen in the examination printouts, demonstrate a somewhat bipeaked superior bundle pattern. These bipeaked patterns strengthen the assumption that a split bundle is a common imaging variant because these normative ranges are based on data from a large group of normal individuals.

Figure 1 shows data from a healthy eye imaged with a GDx variable corneal compensation that demonstrated qualitatively a superior split bundle. Data were exported for various ring diameters, demonstrating that the split bundle phenomenon in this eye seems to become more evident as the measurement ring size increases (as the ring is placed more peripherally).

The imaging data presented so far cannot discriminate whether split bundles are true anatomic variants or perhaps imaging artifacts. To this extent, a histologic approach may assist in addressing the question of whether split bundles indeed are true anatomic variants.

The histologic analysis of the RNFL was performed previously in both primates and humans.[5–10] True measurement values are difficult to obtain using histologic methods, owing to potential shrinkage or expansion of tissues during death, harvesting, and processing.[11] Hence in this study, the authors took a more qualitative look at the peripapillary RNFL thickness pattern, realizing that the measurement

Originally received: July 14, 2006.
Final revision: January 3, 2007.
Accepted: January 6, 2007. Manuscript no. 2006-779.

From the Department of Ophthalmology, Hadassah–Hebrew University Medical Center, Jerusalem, Israel.

Dr Blumenthal received research support from Laser Diagnostics Technologies, San Diego, California. Tissue procured by the National Disease Research Interchange, Philadelphia, Pennsylvania, was used in this study.

Correspondence to Eytan Z. Blumenthal, MD, Department of Ophthalmology, Hadassah University Hospital, P.O. Box 12000, Jerusalem 91120, Israel. E-mail: eytan@blumenthal.org.il.

ISSN 0161-6420/07/$–see front matter
doi:10.1016/j.ophtha.2007.01.028

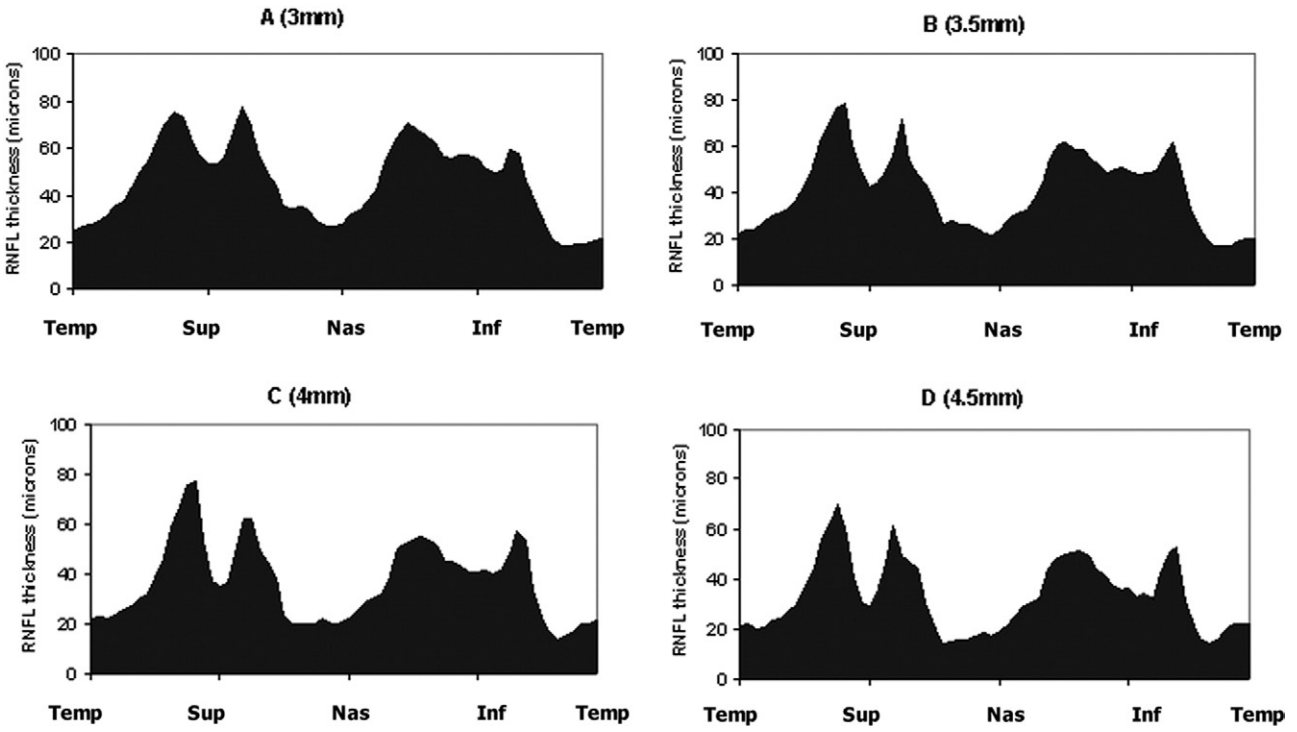

Figure 1. Plots showing exported, postprocessed, GDx variable corneal compensation data from a healthy eye with an apparent superior split bundle pattern. The measurement ring was set to 4 different ring sizes with diameters of (**A**) 3.0 mm, (**B**) 3.5 mm, (**C**) 4.0 mm, and (**D**) 4.5 mm. Note that the split in the superior bundle seems to change somewhat across the different ring diameter plots. Inf = inferior; nas = nasal; RNFL = retinal nerve fiber layer; sup = superior; temp = temporal.

values obtained may prove to be relative rather than absolute values, yet the overall modulation (temporal-superior-nasal-inferior-temporal graph pattern) likely will be relatively conserved. In this study, the authors histologically evaluated 14 healthy human eyes (from 13 subjects), obtained after death, to determine whether split bundle patterns can be identified on histologic evaluation of these tissues.

Materials and Methods

Globes

Fourteen human eyes (from 13 subjects) were obtained for research purposes from an eye bank. Consent for the use of tissues in medical research was obtained from the immediate family. Tissue harvesting was performed according to the regulations for obtaining and handling of human tissue for research purposes and in accordance with the tenets of the Declaration of Helsinki for research involving human subjects. Approval for this study was obtained from the institutional human subject committee. A detailed postmortem history was obtained, in which known eye diseases, previous eye surgery, chronic eye medications, diabetes, or any other systemic diseases that may affect retinal morphologic features were ruled out. Although 1 eye per subject was intended, for 1 individual we unintentionally processed both eyes and decided to present both. These eyes were fixed in 4% buffered formaldehyde a mean±standard deviation of 5.82±2.2 hours (range, 3–10.5 hours) after death. Macroscopic examination of these eyes excluded gross disease.

Tissue Processing and Retinal Nerve Fiber Layer Thickness Measurements

The technique for sectioning the globe was described previously.[12] Briefly, the umbrella technique approach to sectioning the globe provides continuous peripapillary ring-shaped histologic sections at varying diameters. In this study, the processed tissue was serially sectioned into 4-μm thickness ring sections, later identifying those ring sections having a precise diameter of 3.0, 3.5, 4.0, and 4.5 mm by way of measuring the inner circumference. Each of these 4 ring sections was photographed under the microscope using an Olympus BX41 microscope with Olympus DP70 digital camera (Olympus Optical Corporation, Tokyo, Japan). Histologic sections were photographed for diameter measurement using ×20 magnification and ×40 magnification for RNFL thickness measurements. Images were captured onto a personal computer using Olympus DP Controller software, version 1.2.1.108, at 4080×3072 pixel resolution, camera shutter speed of 1/900 seconds, and ISO-200

Table 1. Demographics of the Patients Studied

Age, mean±standard deviation (range), yrs	65.7±7.7 (51–80)
Gender, male/female	8 (61%)/5 (39%)
Eye, right/left	7 (50%)/7 (50%)
Cause of death	
Vascular	7 (54%)
Neoplastic	4 (31%)
Other	2 (15%)
Ethnicity	
White	12 (92%)
Black	1 (8%)

Table 2. Prevalence of Split Bundle Patterns According to the Examiners*

Examiner	Definite Split Bundle Pattern	Borderline Split Bundle Pattern	No Split Bundle Pattern
A	6/28	5/28	17/28
B	7/28	2/28	19/28
C	5/28	3/28	20/28
Uniform agreement	5/28	0/28	16/28

K value for examiners A and B, 0.79; examiners A and C, 0.57; examiners B and C, 0.61.
*Fourteen eyes included; data presented for 28 hemispheres (superior and inferior hemisphere for each eye).

exposure. Images were captured with a calibrated digital millimeter scale integrated into the captured images.

From each digitized section, 100 equidistant RNFL thickness measurements along the inner circumference were made, according to the technique previously described.[12] These 100 equidistant RNFL thickness measurements were collected from the circumference of each ring section, conforming to the temporal-superior-nasal-inferior-temporal orientation.

Assessing Split Bundle Patterns

Three observers, masked to each other's results, viewed an overlay of the 4 plots originating from each eye (3.0-, 3.5-, 4.0-, and 4.5-mm diameter ring sections) and determined whether a split bundle pattern was evident. Each observer qualitatively scored the superior and inferior aspects of each eye as either definite split

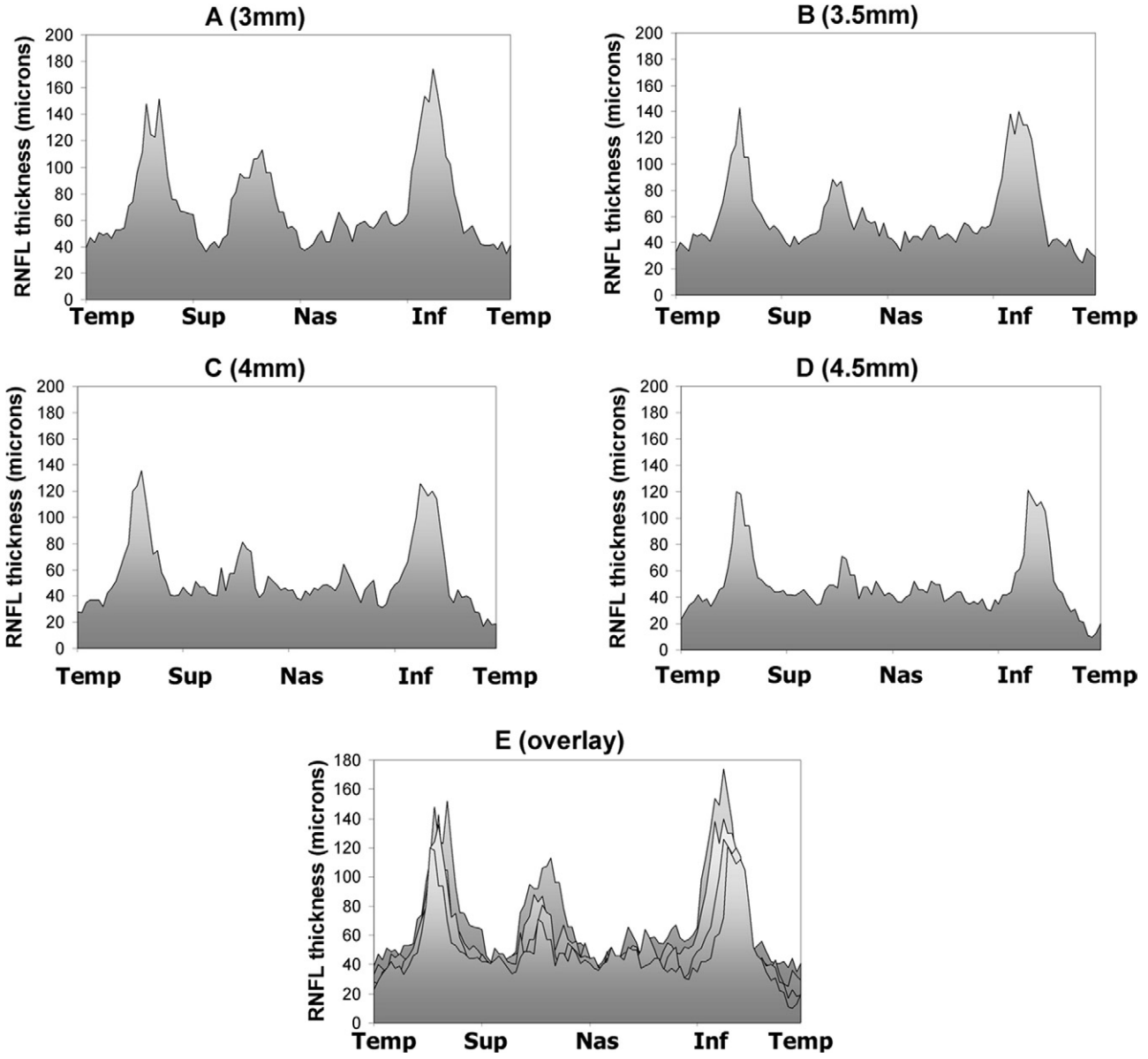

Figure 2. Plots showing histologic data of an eye demonstrating a superior split bundle. Retinal nerve fiber layer (RNFL) thickness measurements are presented for ring sections with diameters of (**A**) 3.0 mm, (**B**) 3.5 mm, (**C**) 4.0 mm, (**D**) 4.5 mm, and (**E**) an overlay of plots A through D. Inf = inferior; nas = nasal; sup = superior; temp = temporal.

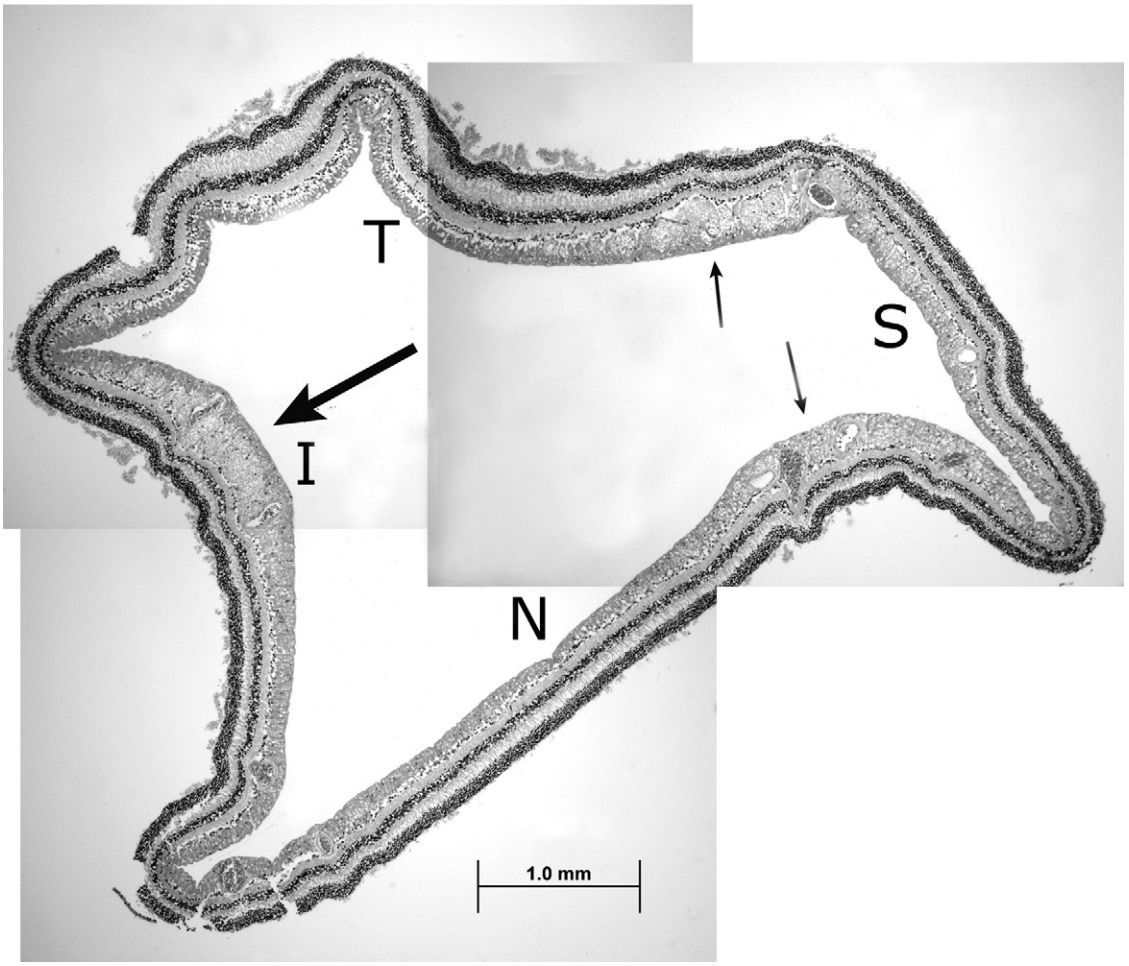

Figure 3. Photomicrograph showing a 3.0-mm diameter circumferential peripapillary histologic section of the eye shown in Figure 4 demonstrating a superior split bundle (thin arrows) and a single inferior bundle (thick arrow). I = inferior; N = nasal; S = superior; T = temporal.

bundle pattern, borderline split bundle, or no split bundle. A borderline split bundle pattern was given to patterns, judged by each observer independently, as presenting a mild or incomplete form of split. Interobserver agreement was assessed using a pairwise κ statistic to enable a separate comparison of each observer with the other 2 observers and was controlled for multiple comparisons using the Bonferroni method. An overall consensus decision for the presence of a split bundle was determined using the following rule, chosen a priori: only eyes in which all 3 observers independently gave a score of definite split bundle pattern to the same hemisphere (be it superior or inferior) were considered to have definite split bundle.

Results

Table 1 presents the demographic characteristics of the studied eyes. According to the subjective judgment of 3 observers, the prevalence of definite split bundles in this study was 36% (5/14) of the eyes, of which 3 were found superiorly and 2 inferiorly. None of these 14 eyes demonstrated both a definite superior and a definite inferior split bundle. Incidentally, the single subject in whom both eyes were entered into the study did not show a split bundle pattern in either eye. Table 2 presents the 3 examiners' scores. Interobserver agreement coefficients (κ) for a comparison between each pair of observers (Table 2) were 0.57, 0.61, and 0.79 ($P<0.001$ for all comparisons). Each of these pairwise comparisons was found to be statistically significant, even after correcting for multiple comparisons, using the Bonferroni method (a corrected significance threshold; $P<0.016$).

Figure 2 shows an example of an eye that was agreed on by all 3 examiners to have a typical split superior bundle. The RNFL thickness measurements are presented for ring sections of increasing diameters. Figure 3 shows the 3.0-mm diameter circumferential peripapillary histologic section of the eye shown in Figure 2. Figure 4 presents, as an example, plots of eyes demonstrating definite, borderline, and no split bundle patterns. All examples chosen for this figure are from cases in which there was a uniform agreement among the 3 observers, except for the 1 example of a borderline split in which 2 of 3 observers were in agreement.

Discussion

Split bundle patterns, appearing either superiorly, inferiorly, or both, have been described as an imaging observation using both scanning laser polarimetry and optical coherence tomography technology.[3,4] Moreover, pooled normative database data from these 2 methods seems to suggest that such

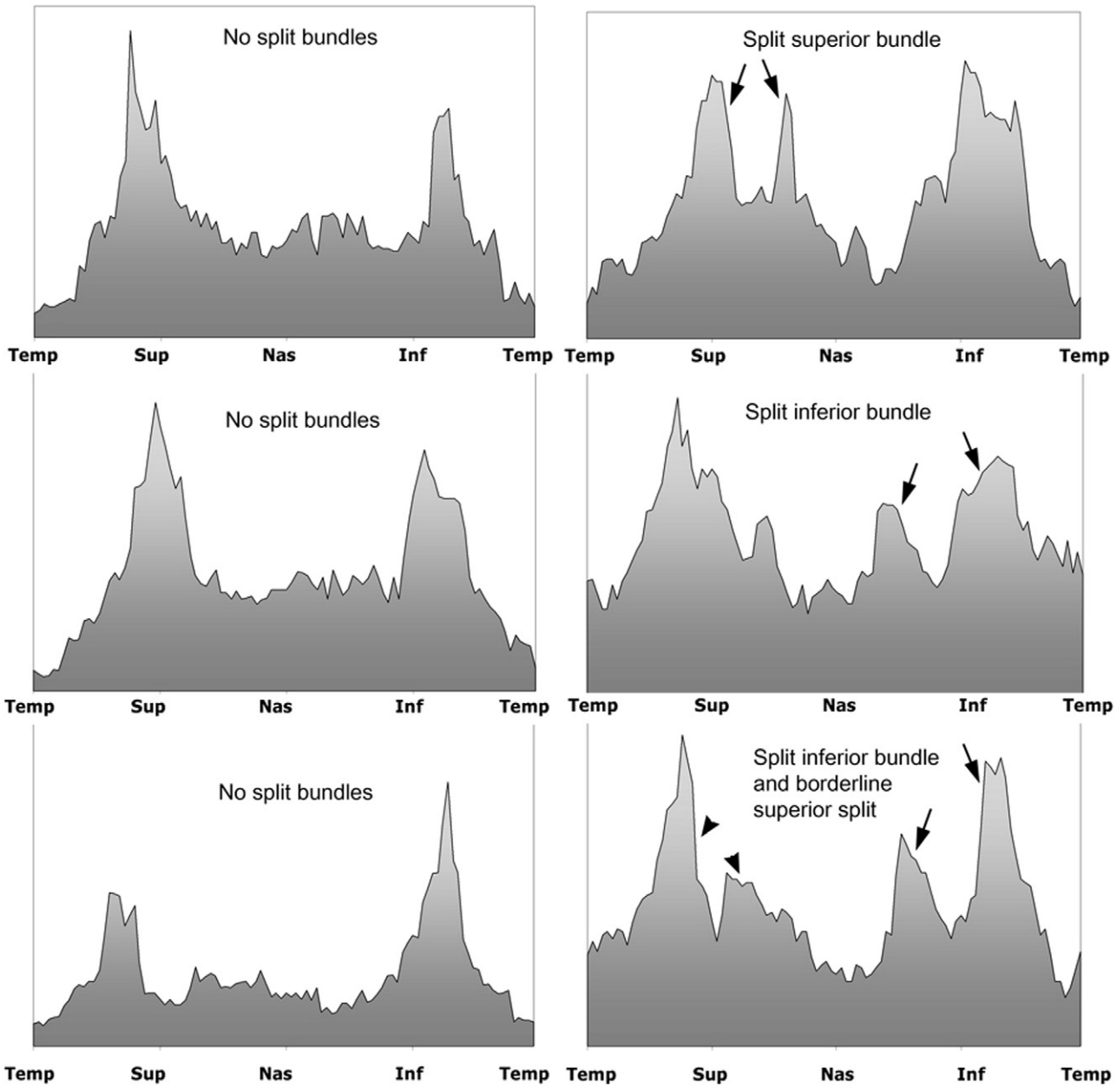

Figure 4. Plots from 6 eyes demonstrating the patterns discussed in this study. **Left**, Eyes with no split bundle pattern. **Top right**, Definite superior split. **Center right**, Definite inferior split. **Bottom right**, Combined borderline superior split and definite inferior split (all plots in this figure are from 3.5-mm-diameter rings). Inf = inferior; nas = nasal; sup = superior; temp = temporal. Arrows, definite split; arrowheads, borderline split.

splitting may be a common variant. The fact that such split appears on 2 distinct imaging methods that have little in common in terms of the physics underlying the image acquisition process strengthens the possibility that such splitting may represent a true anatomic variant.

In this study, the authors investigated the presence of split bundles histologically on a group of 14 postmortem eyes. These postmortem eyes were considered healthy based on a detailed postmortem history, and therefore the authors could not rule out entirely the presence of ophthalmic disease. The histologic methodology used in this study is exposed to several potential artifacts because of delayed fixation and tissue processing, which are common to other histologic techniques.[12–14] These artifacts may result in unexpected RNFL thickness changes. The authors expect these limitations to have a relatively uniform effect around the RNFL circumference, and hence qualitative results pertaining to shape are likely less influenced than quantitative measurements. This study is not powered to investigate specific associations between various clinical and demographic characteristics and the existence of split bundle patterns. Likewise, data on 14 eyes of 13 subjects are not sufficient to estimate reliably average split patterns across the general population.

The authors found a relatively high proportion of eyes demonstrating definite split bundles, a higher frequency than was found by Colen and Lemij[3] in their GDx fixed corneal compensation article. The presence of a split bundle seems to be a relatively common normal variant and must not be confused with the wedge-shaped RNFL loss that can be found in glaucomatous optic neuropathy.

References

1. Essock EA, Sinai MJ, Bowd C, et al. Fourier analysis of optical coherence tomography and scanning laser polarimetry retinal nerve fiber layer measurements in the diagnosis of glaucoma. Arch Ophthalmol 2003;121:1238–45.
2. Leung CK, Chan WM, Chong KK, et al. Comparative study of retinal nerve fiber layer measurement by StratusOCT and GDx VCC. I: correlation analysis in glaucoma. Invest Ophthalmol Vis Sci 2005;46:3214–20.
3. Colen TP, Lemij HG. Prevalence of split nerve fiber layer bundles in healthy eyes imaged with scanning laser polarimetry. Ophthalmology 2001;108:151–6.
4. Pieroth L, Schuman JS, Hertzmark E, et al. Evaluation of focal defects of the nerve fiber layer using optical coherence tomography. Ophthalmology 1999;106:570–9.
5. Dichtl A, Jonas JB, Naumann GO. Retinal nerve fiber layer thickness in human eyes. Graefes Arch Clin Exp Ophthalmol 1999;237:474–9.
6. Morgan JE, Waldock A, Jeffery G, Cowey A. Retinal nerve fibre layer polarimetry: histological and clinical comparison. Br J Ophthalmol 1998;82:684–90.
7. Ogden TE. Nerve fiber layer of the primate retina: thickness and glial content. Vision Res 1983;23:581–7.
8. Quigley HA, Addicks EM. Quantitative studies of retinal nerve fiber layer defects. Arch Ophthalmol 1982;100:807–14.
9. Radius RL. Thickness of the retinal nerve fiber layer in primate eyes. Arch Ophthalmol 1980;98:1625–9.
10. Varma R, Skaf M, Barron E. Retinal nerve fiber layer thickness in normal human eyes. Ophthalmology 1996;103:2114–9.
11. Frenkel S, Morgan JE, Blumenthal EZ. Histological measurement of retinal nerve fibre layer thickness. Eye 2005;19:491–8.
12. Blumenthal EZ. Quantifying retinal nerve fiber layer thickness histologically: a novel approach to sectioning of the retina. Invest Ophthalmol Vis Sci 2004;45:1404–9.
13. Balazsi AG, Rootman J, Drance SM, et al. The effect of age on the nerve fiber population of the human optic nerve. Am J Ophthalmol 1984;97:760–6.
14. Abramson DH, Schefler AC, Almeida D, Folberg R. Optic nerve tissue shrinkage during pathologic processing after enucleation for retinoblastoma. Arch Ophthalmol 2003;121:73–5.